Similar Molecular Interactions of Factor VII and Factor VIIa with the Tissue Factor Region that Allosterically Regulates Enzyme Activity

Robert F. Kelley,* Jihong Yang, Charles Eigenbrot, Paul Moran, Mark Peek, Michael T. Lipari, and Daniel Kirchhofer

Departments of Protein Engineering and Physiology, Genentech Inc., 1 DNA Way, South San Francisco, California 94080

Received September 25, 2003; Revised Manuscript Received December 8, 2003

ABSTRACT: Tissue factor (TF) binds the zymogen (VII) and activated (VIIa) forms of coagulation factor VII with high affinity. The structure determined for the sTF−VIIa complex [Banner, D. W., et al. (1996) *Nature 380*, 41−46] shows that all four domains of VIIa (Gla, EGF-1, EGF-2, and protease) are in contact with TF. Although a structure is not available for the TF−VII complex, the structure determined for free VII [Eigenbrot, C., et al. (2001) *Structure 9*, 675−682] suggests a significant conformational change for the zymogen to enzyme transition. In particular, the region of the protease domain that must contact TF has a conformation that is altered from that of VIIa, suggesting that the VII protease domain interacts with TF in a manner different from that of VIIa. To test this hypothesis, a panel of 12 single-site sTF mutants, having substitutions of residues observed to contact the proteolytic domain of VIIa, have been evaluated for binding to both zymogen VII and VIIa. Affinities were determined by surface plasmon resonance measurements using a noninterfering anti-TF monoclonal antibody to capture TF on the sensor chip surface. Dissociation constants (K_D) measured for binding to wild-type sTF are 7.5 ± 2.4 nM for VII and 5.1 ± 2.3 nM for VIIa. All of the sTF mutants except S39A and E95A exhibited a significant decrease (>2-fold) in affinity for VIIa. The changes in affinity measured for VII or VIIa binding with substitution in sTF were comparable in magnitude. We conclude that the proteolytic domain of both VII and VIIa interacts with this region of sTF in a nearly identical fashion. Therefore, zymogen VII can readily adopt a VIIa-like conformation required for binding to TF.

Coagulation upon vascular damage in vertebrates is initiated when blood contacts the integral membrane protein tissue factor (TF)[1] expressed on cells surrounding the vasculature (*1*). TF initiates a cascade of proteolytic events ultimately resulting in activation of prothrombin to thrombin which converts fibrinogen to fibrin (*2*). Fibrin polymerizes to form the meshwork of a clot. TF initiates coagulation through its role as the obligate cofactor for serine protease coagulation factor VIIa (VIIa). Binding of VIIa to TF is required for full enzymatic activity (*3*). Factor VIIa in plasma is found predominately in the zymogen or inactive, single-chain form (VII), with only ∼1% present as the active, two-chain polypeptide (VIIa) (*4*). Calcium-dependent binding of VII to TF promotes the activation of VII through proteolytic cleavage of the Arg152−Ile153 peptide bond. Activation is catalyzed by many proteases *in vitro*, but the most efficient catalyst *in vivo* is probably Xa (*5*). Autocatalytic activation of VII by the TF−VIIa complex may be important in the initiation stage of coagulation.

TF promotes the enzymatic activity of VIIa through an allosteric linkage that fosters formation of the active site (*6*) and by providing contacts for the physiological substrates, IX and X (*7*). The allosteric linkage is most apparent in the TF-dependent increase in the amidolytic activity of VIIa against synthetic peptidyl substrates (*8*, *9*). The structure determined for the TF−VIIa complex containing a covalent active site inhibitor shows that the active site of VIIa is distant from the TF contact region (*10*). The TF binding surface involves all of the domains of VIIa (Gla, EGF-1, EGF-2, and protease). The TF−protease contact region is presumed to be important for the allosteric linkage to the active site since mutations on VIIa in this interface result in weakened enhancement of amidolytic function upon TF binding (*11*). Additional TF residues that are important for full enzymatic activity with the macromolecular substrates are found on the C-terminal domain of TF, outside of the interface with VIIa (*7*).

A structure of a truncated form of VII comprising only the EGF2 and catalytic domains (rF7) has recently been determined by X-ray crystallography (*12*). Crystals were obtained in the presence of an exosite peptide inhibitor but without TF or an active site inhibitor bound. Although the rF7 construct included the Arg152 activation cleavage site, the crystals only contained uncleaved protein. Further analysis of the structure suggested that the protein had crystallized in the zymogen conformation as indicated by the improper formation of the S1 binding pocket. β-Strand B2 (residues 153−162) was also shifted three amino acids from its position in the TF−VIIa complex, and the conformation of the region on the protease domain that contacts

* To whom correspondence should be addressed: Department of Protein Engineering MS #27, Genentech Inc., 1 DNA Way, South San Francisco, CA 94080. Phone: (650) 225-2321. Fax: (650) 225-3734. E-mail: rk@gene.com.

[1] Abbreviations: TF, tissue factor; sTF, soluble tissue factor (residues 1−219); VII and VIIa, factor VII and factor VIIa, respectively; IX and IXa, factor IX and factor IXa, respectively; X and Xa, factor X and factor Xa, respectively; Gla, γ-carboxyglutamic acid; EGF, epidermal growth factor; SPR, surface plasmon resonance.

10.1021/bi035738i CCC: $27.50
Published on Web 01/16/2004

TF was quite different. These conformational changes may be important for the allosteric linkage between TF binding and enzymatic activity. Modeling of the rF7 structure onto the structure determined for the sTF−VIIa complex revealed a steric clash between the protease domain of zymogen VII and the N-terminal fibronectin type III domain of TF. This suggests that VII may interact with this region of TF in a manner different from that of VIIa. If this hypothesis is correct, then mutations in this region of sTF should have different effects on binding of VII and VIIa. To test this hypothesis, we have measured the affinities for both VII and VIIa binding to a panel of sTF mutants. These mutant proteins comprise amino acid changes in the N-terminal domain of TF that is in contact with the protease domain of VIIa in the TF−VIIa structure. We find that substitutions in TF in this region have nearly identical consequences for binding of VII and VIIa.

MATERIALS AND METHODS

Reagents. Purified human recombinant VII, expressed in human 293 cells, was a gift from Mark O'Connell (Genentech Inc.) and was described recently (*13*). Xa was from Haematologic Technologies Inc. (Essex Junction, VT). Chromozym-tPA was from Boehringer Mannheim (Indianapolis, IN). The monoclonal anti-TF antibody 5G6 was described previously (*14*) and binds to TF outside the TF−VIIa binding region. Kunitz domain inhibitor IV-49-C (*15*) was the kind gift of M. Dennis (Genentech Inc.). Fatty acid-free BSA was from Calbiochem (La Jolla, CA). Dioleoyl 1,2-diacyl-*sn*-glycero-3-(phospho-L-serine) (PS) and oleoyl 1,2-diacyl-*sn*-glycero-3-phosphocholine (PC) were from Avanti Polar Lipids Inc. (Alabaster, AL).

Site-Directed Mutagenesis, Expression, and Purification of Soluble TF (sTF) Mutants. Expression of sTF(1−219) mutants in *Escherichia coli* and subsequent purification on a D3 antibody affinity column were carried out as described previously (*16*). Protein concentrations were determined by absorbance measurements using an ϵ_{280} of 29.4 mM^{-1} cm^{-1} calculated from quantitative amino acid analysis data.

Purification of VII. To remove the VIIa content (10−20%) of VII preparations, they were incubated with a 20-fold molar excess of biotin-X-FPR chlormomethyl ketone (Haematologic Technologies) in 20 mM Tris-HCl (pH 8.0), 150 mM NaCl, and 5 mM $CaCl_2$ for 2 h. Additional biotin-X-FPR chlormomethyl ketone was added (20-fold molar excess) and the mixture incubated overnight. The reaction mixture was dialyzed extensively against 20 mM Tris-HCl (pH 8.0), 150 mM NaCl, and 5 mM $CaCl_2$ using a 10 kDa cutoff dialysis cassette (Pierce, Rockford, IL) and then incubated with avidin agarose resin (Sigma, St. Louis, MO) overnight at 4 °C. After a brief centrifugation, the supernatant was collected and the protein analyzed by SDS−PAGE using a 4 to 20% gradient Tris-glycine gel (Invitrogen, Carlsbad, CA). The protein concentration was determined by quantitative amino acid analysis. The functional integrity of the thus purified VII was verified by an X activation assay with relipidated recombinant TF(1−243) (*7*). The initial rates of X activation by the purified VII were indistinguishable from those of fully converted VIIa, indicating that VII is converted into a fully active enzyme.

Amidolytic Activity of the Soluble TF−VIIa Complex. Measurements of the amidolytic activity of the complexes formed between VIIa and wild-type or mutant sTF were performed as described previously (*7*, *14*) using Chromozym-tPA as the substrate.

Activation of X by the Soluble TF−VIIa Complex. This assay was carried out essentially as described previously (*7*, *14*). Phospholipid vesicles were prepared (*17*) using oleoyl 1,2-diacyl-*sn*-glycero-3-phosphocholine (PC) and dioleoyl 1,2-diacyl-*sn*-glycero-3-(phospho-L-serine) (PS) (7:3 molar ratio). The PC/PS vesicles together with VIIa and increasing concentrations of sTF mutants were incubated for 20 min in HBSA buffer. The reaction was started by adding X. The concentrations of the reactants in this mixture were as follows: 0.1 nM VIIa, 0.5 mM PCPS, 200 nM X, and 0.25−256 nM sTF mutant. Aliquots (50 μL) of the reaction mixture were taken at different time points up to 2 min and the reactions quenched in 150 μL of 20 mM EDTA. After addition of 50 μL of 1.5 mM S2765, the increase in absorption at 405 nm measured on a kinetic microplate reader (Molecular Devices) and the linear rates of Xa generation were calculated. The data were fit to a four-parameter equation using Kaldeidagraph 3.6 (Synergy Software, Reading, PA), and the maximal velocities (v_{max}) as well as the sTF mutant concentrations that gave 50% of v_{max} (EC_{50}) were determined.

Determination of Binding Constants for Binding of VII and VIIa to sTF Mutants. Binding affinities were determined by surface plasmon resonance (SPR) measurements on a BIAcore 3000 instrument (Biacore, Inc.). Monoclonal anti-TF antibody 5G6 was immobilized at a density of 6000−8000 resonance units (RU) on all four flow cells of a Pioneer B1 sensor chip. Immobilization was achieved by random coupling through amino groups using a protocol described by the manufacturer. Wild-type or mutant sTF was captured on flow cells 2−4 at a level of 200−300 RU, whereas flow cell 1, containing only the antibody, was used as the reference cell. Sensorgrams were recorded for binding of VII and VIIa to these surfaces by injection of a series of solutions ranging in concentration from 12.5 to 400 nM in 2-fold increments. The signal from the reference cell for the same injection was subtracted from the observed sensorgram. At the end of each sensorgram, bound VII or VIIa was eluted by injection of 50 mM EDTA. In these measurements, data were collected for the complete zymogen series before injections of the activated enzyme were made. Kinetic constants were calculated by nonlinear regression analysis of the data according to a 1:1 binding model using software supplied by the manufacturer. Upon completion of the VII and VIIa binding series, the antibody-bound sTF was eluted with 10 mM HCl. The antibody surfaces were then reused for binding analysis using a different set of sTF mutants.

RESULTS

Selection of TF Mutants. Residues on TF were chosen for mutagenesis on the basis of their proximity to the protease domain of VIIa in the sTF−VIIa complex structure. The 12 residues that were selected (Q37, S39, G43, D44, W45, R74, F76, Y78, E91, Y94, E95, and N96) form a contiguous patch on the N-terminal fibronectin type III domain of TF (Figure 1A). This surface is in intimate contact with the protease domain of VIIa in the TF−VIIa complex (*10*). Modeling

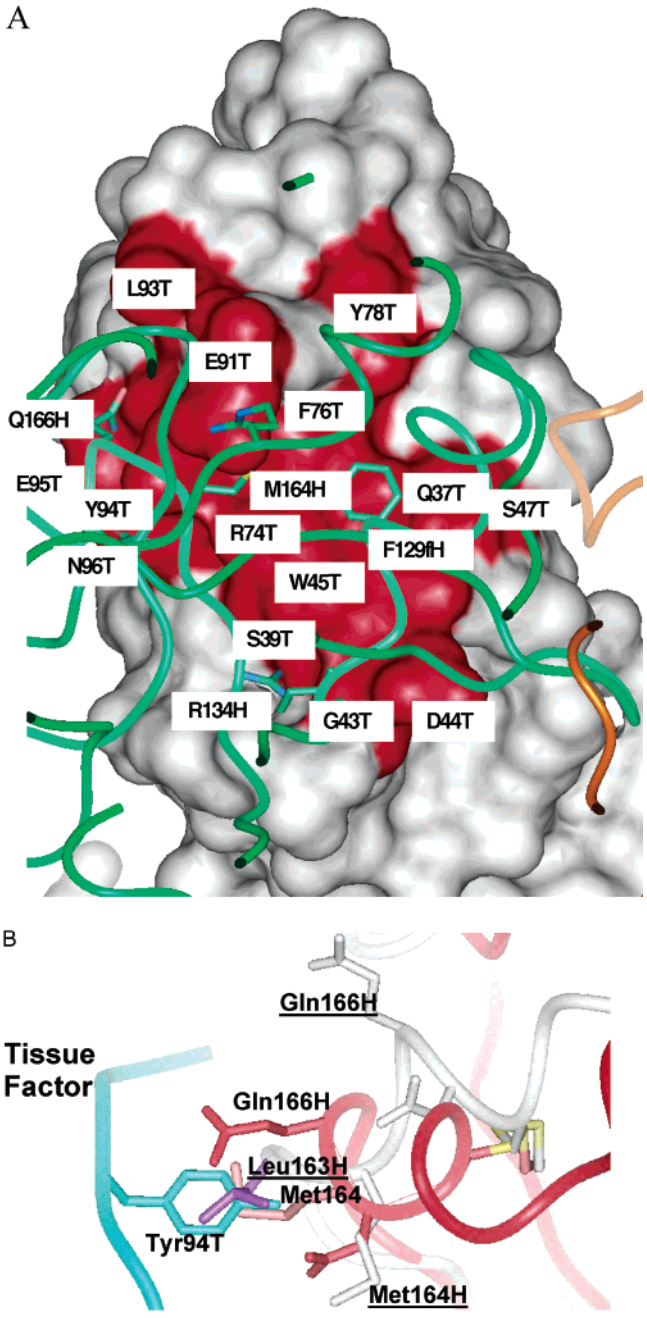

FIGURE 1: Structure of the interface between TF and the proteolytic domain of VIIa. (A) Contact region defined by Banner et al. (*10*) between sTF (space filling model) and the VIIa proteolytic domain (green ribbon). Residues on sTF mutated in this study are labeled with a T suffix; residues from the VIIa proteolytic domain have an H suffix and are numbered on the basis of the alignment with chymotrypsin. (B) Superposition of structures determined for zymogen VII (white ribbon) and the sTF−VIIa complex (red ribbon for VIIa and aqua ribbon for sTF). Side chains from zymogen VII that would be in steric conflict with TF residue Tyr94 are colored purple. Labels for zymogen VII side chains are underlined.

studies suggest a steric hindrance between this patch and the protease domain of VII; for example, Leu163 of VII would clash with Tyr94 of TF (Figure 1B). The 12 residues on TF, with the exception of W45, were individually substituted with alanine. Since the W45A mutant was poorly expressed, a Phe substitution at this position was used. Two residues that do not contact VIIa but are adjacent to this patch, Ser47 and Leu93, were also chosen for alanine substitution.

Table 1: Factor X Activation[a]

	EC_{50} (sTF, nM)	EC_{50} ratio (sTF_{mut}/sTF_{wt})	υ_{max} ratio (sTF_{mut}/sTF_{wt})
wild type	2.0 ± 0.5	1.0	1.0
Q37A	44.6 ± 16.6	22.3 ± 7.2	1.0 ± 0.1
S39A	3.4 ± 0.9	1.7 ± 1.0	1.3 ± 0.2
G43A	8.6 ± 3.0	4.3 ± 2.0	1.3 ± 0.3
D44A	68.4 ± 17.4	34.8 ± 1.5	0.9 ± 0.1
W45F	111.4 ± 13.8	61.6 ± 10.5	0.9 ± 0.2
S47A	1.7	0.9	0.8
R74A	ND[b]	ND[b]	ND[b]
F76A	103.0 ± 47	52.0 ± 25.1	1.0 ± 0.2
Y78A	12.1 ± 4.8	5.3 ± 0.9	1.0 ± 0.1
E91A	78.3 ± 22.6	34.9 ± 0.8	0.9 ± 0.01
L93A	2.0	0.7	1.0
Y94A	59.9 ± 39.6	26.0 ± 11.7	1.0 ± 0.2
E95A	1.0 ± 0.3	0.6 ± 0.3	0.9 ± 0.2
N96A	12.5 ± 3.5	8.3 ± 4.7	0.8 ± 0.1

[a] The values are the averages ± the standard deviation from three or more experiments, except for the values for S47A and L93A which are the average of two experiments. [b] Not determined.

Cofactor Function of sTF Mutants for X Activation. The ability of the sTF mutants to support the enzymatic activity of VIIa was examined using X as the substrate. These experiments used a fixed concentration of VIIa, X, and phospholipids but a varied concentration of the sTF mutant. Initial rates of Xa generation were determined, and the dependence on sTF concentration was analyzed using a four-parameter equation to yield the υ_{max} and EC_{50} values given in Table 1. All of the mutants except S39A, S47A, L93A, and E95A gave a significant increase in the concentration (EC_{50}) of sTF required to produce 50% of the total change in υ_{max}. The increase in EC_{50} primarily reflects a decrease in the affinity of VIIa for the sTF mutant. Upon saturation of VIIa with sTF, all of the mutants were equivalent to the wild type in supporting VIIa-catalyzed cleavage of X as indicated by the υ_{max} values. Similarly, in experiments with the peptide substrate Chromozym-tPA, the mutants stimulated the amidolytic activity of VIIa to the same extent as wild-type sTF when the enzyme was saturated with the cofactor (data not shown).

Preparation of Zymogen VII. A preparation of VII free of VIIa was needed to compare the binding epitopes on sTF for VII and VIIa. However, most preparations of zymogen from plasma or recombinant sources are contaminated with VIIa. The reactivity of the enzyme toward active site chloromethyl ketone inhibitors (*18*) could be exploited to remove VIIa from recombinant VII. By using a biotinylated chloromethyl ketone inhibitor, the active site-modified VIIa could be removed on an avidin column. As shown by SDS−PAGE on reduced samples (Figure 2), the VIIa contaminant (two bands with molecular weights of approximately 25 000 and 32 000) in the VII preparation was completely removed by the biotin−avidin procedure, resulting in homogeneous, single-chain VII with an apparent MW of 50 000. Zymogen VII prepared in this fashion is stable and does not autoactivate during storage at −20 °C but can be activated by Xa to yield the fully active enzyme (data not shown).

Affinity of sTF for VII and VIIa. We have previously used SPR to measure VIIa affinities for a panel of alanine mutants of sTF by using a biotinylated active site inhibitor of VIIa for the site-specific immobilization of VIIa on the sensor chip surface (*16*). Binding of active site inhibitors is known

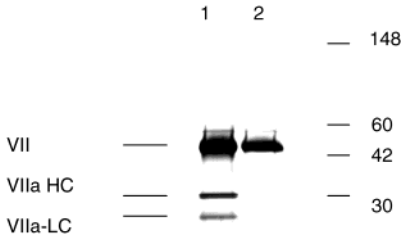

FIGURE 2: Preparation of zymogen VII. SDS−PAGE assay of removal of VIIa from the VII preparation by chromatography on avidin agarose following reaction with biotin-X-FPR chloromethyl ketone: VII before (lane 1) and after (lane 2) treatment to remove VIIa.

to influence the affinity of VIIa for TF (*19*), and zymogen VII reacts poorly with the active site inhibitor. Direct coupling of VIIa via amino groups has been shown to hinder TF binding (*20*), and immobilization of each sTF mutant would require standardization of multiple chip surfaces. Thus, we have employed an alternative immobilization strategy in which a non-neutralizing monoclonal antibody is used to capture wild-type or mutant sTF and then binding of VII or VIIa to these surfaces is measured. The monoclonal anti-TF antibody 5G6 (*14*) used for these experiments binds to an epitope distinct from the VIIa binding site and similar to that determined by X-ray crystallography for the D3H44−sTF complex (*21*). In experiments where sTF was immobilized on the sensor chip surface, prebinding of 5G6 caused only a small increase (from 13.6 to 16.9 nM) in the K_D for VIIa binding. Binding of 5G6 has no significant effect on the amidolytic activity of VIIa in complex with wild-type (*14*) or mutant sTF (data not shown). Mab 5G6 does inhibit the activity of the TF−VIIa complex toward macromolecular substrates X and IX (*7*) and blocks autoactivation of VII (D. Kirchhofer, unpublished results). The K_D measured for 5G6−sTF binding by SPR is 1.7 nM, and most importantly, the k_{off} is 4-fold slower than that measured for the sTF−VIIa complex (*14*). Under the experimental conditions of high-density 5G6 immobilization with a small amount of sTF captured, the binding kinetics reflect the sTF−VII or −VIIa interaction and not dissociation of sTF from the antibody.

Typical sensorgrams observed for binding of VIIa or VII to wild-type sTF, immobilized via binding to 5G6, are shown in panels A and B of Figure 3, and the results of an analysis according to a 1:1 binding model are summarized in Table 2. The kinetic constants and the K_D value determined for VIIa binding agree with previous results obtained using active site-immobilized VIIa (*16*). Zymogen VII binds to wild-type sTF with an affinity only 1.5-fold weaker than that measured for VIIa. The small change in affinity primarily reflects an increased off-rate for VII, whereas the on-rates measured for the two proteins are not significantly different.

Although sTF is a poor cofactor for autoactivation of VII in the absence of high concentrations of phospholipids and VIIa (*22*), it is possible that activation of VII to VIIa does occur on the sensor chip surface, leading to apparent similar affinities of VII and VIIa for sTF. To test this possibility, we examined binding of a Kunitz domain active site inihibitor to the ternary complexes of the 5G6−sTF complex and VII or VIIa. Kunitz domain inhibitors usually bind tightly to activated serine proteases and only weakly to the zymogen forms (*23*). Since the Kunitz domain has an approximately

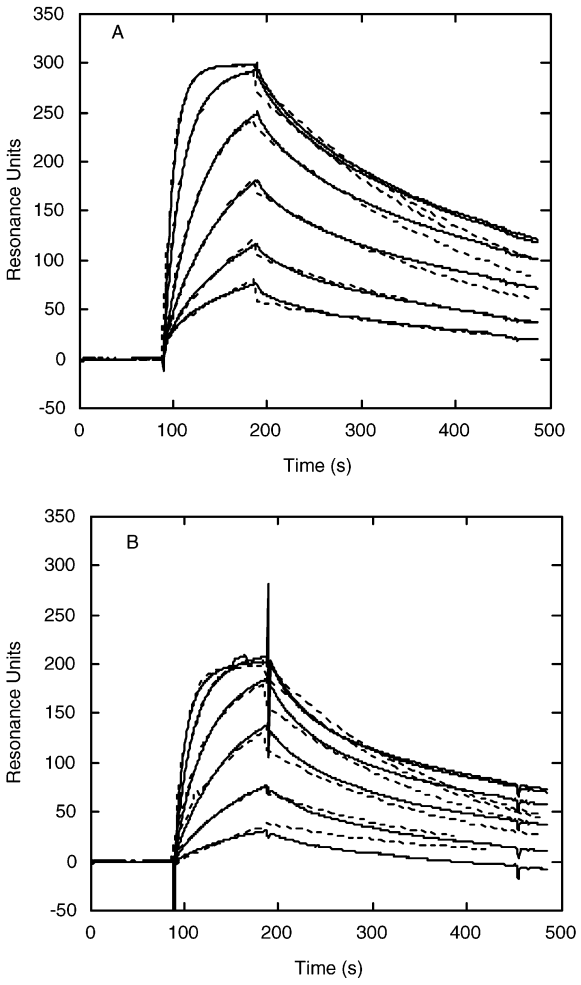

FIGURE 3: Surface plasmon resonance (SPR) measurements of VIIa (A) or zymogen VII (B) binding to sTF. Monoclonal antibody 5G6 was used to capture sTF on the sensor chip surface, and then binding data were collected for six different concentrations of VII or VIIa. The value from a reference cell having only the immobilized antibody was subtracted from the data to yield the sensorgrams that are shown. Solid lines depict experimental data, and dashed lines are the result of a simultaneous fit of the data for the six concentrations to a 1:1 binding model.

10-fold lower mass than VIIa, and would produce a smaller SPR signal, we used a higher-density surface in which ~1000 RU of sTF was bound to the antibody. If autoactivation does occur during the binding measurements, then the higher-density surface should promote that reaction. Strong binding was detected for the Kunitz domain with the 5G6−sTF−VIIa complex, as indicated by the positive SPR signal shown in Figure 4. At approximately the same level of complex formation, no Kunitz domain binding was detected with the 5G6−sTF−VII complex (Figure 4). These results suggest that VII does not become activated to VIIa during the binding measurements.

Effects of sTF Mutations on VII and VIIa Affinity. All of the substitutions in the VIIa contact region, with the exception of S39A and E95A, gave significant (>2-fold) decreases in the affinity for both VII and VIIa (Table 2 and Figure 5). For mutants examined previously using active site-immobilized VIIa (*16*) (Q37A, D44A, W45F, and Y94A), a comparable loss of VIIa affinity was determined by using the capture method with 5G6. For the entire set of 12 sTF mutants, changes in affinity for VII and VIIa were

Table 2: Binding of VII and VIIa to 5G6-Captured sTF[a]

	VII			VIIa		
	k_a ($\times 10^{-5}$ M^{-1} s^{-1})	k_d ($\times 10^3$ s^{-1})	K_D (nM)	k_a ($\times 10^{-5}$ M^{-1} s^{-1})	k_d ($\times 10^3$ s^{-1})	K_D (nM)
wild type	7.7 ± 2.1	5.6 ± 1.4	7.5 ± 2.3	5.6 ± 1.5	2.6 ± 0.4	5.1 ± 2.3
Q37A	1.9 ± 0.6	5.4 ± 0.6	31 ± 10	1.9 ± 0.1	8.0 ± 0.7	41.3 ± 1.0
S39A	5.8 ± 1.6	6.9 ± 0.9	12.3 ± 2.3	6.1 ± 0.6	3.3 ± 0.4	5.5 ± 0.2
G43A	2.7 ± 0.4	6.7 ± 0.6	25.2 ± 1.4	3.9 ± 0.3	5.7 ± 1.4	14.6 ± 2.5
D44A	1.4 ± 0.4	4.2 ± 0.5	32.3 ± 8.7	2.3 ± 0.4	8.2 ± 1.8	35.5 ± 2.0
W45F	1.4 ± 0.6	6.2 ± 0.3	53 ± 27	1.9 ± 0.1	10.4 ± 4.7	56 ± 27
R74A	2.0 ± 0.2	7.9 ± 0.9	39.3 ± 5.3	2.3 ± 0.7	8.1 ± 3.5	35.0 ± 6.8
F76A	1.3 ± 0.4	7.0 ± 0.7	57 ± 19	1.8 ± 0.1	8.9 ± 2.9	50 ± 17
Y78A	2.2 ± 0.1	6.2 ± 0.5	28.1 ± 2.7	3.3 ± 0.5	6.7 ± 0.1	20.6 ± 2.5
E91A	1.4 ± 0.3	5.2 ± 0.9	37.4 ± 2.2	2.6 ± 0.4	15.2 ± 3.8	57 ± 6
Y94A	1.2 ± 0.2	5.7 ± 0.5	48 ± 12	2.6 ± 0.3	16.7 ± 4.5	66 ± 23
E95A	4.4 ± 0.1	6.9 ± 0.1	15.7 ± 0.3	5.3 ± 0.3	4.5 ± 0.3	8.5 ± 0.4
N96A	1.3 ± 0.2	6.5 ± 0.9	51 ± 12	2.5 ± 0.2	11.7 ± 1.5	47.1 ± 2.7

[a] Values are the means ± the standard deviation of three or more determinations.

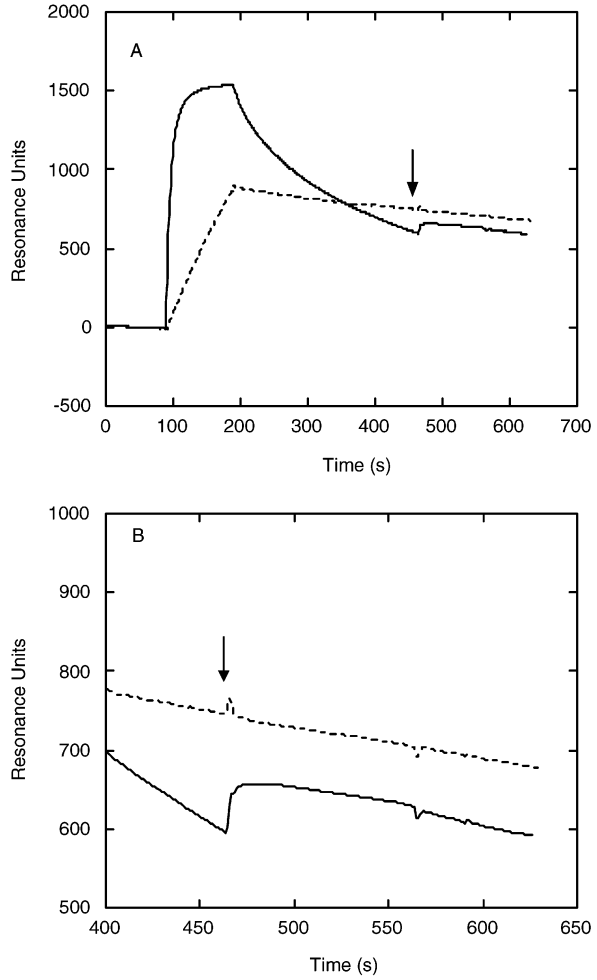

FIGURE 4: Kunitz domain (IV-49-C) binding to the 5G6−sTF−VIIa (—) or 5G6−sTF−VII (- - -) ternary complex. An aliquot of a 1 μM solution of VIIa or 2.5 μM VII was injected onto the sensor chip surface containing the 5G6−sTF complex; dissociation was allowed to occur for 180 s, and then an aliquot of a 50 μM solution of the IV-49-C Kunitz domain (*15*) was injected (indicated by the arrow). The section of the sensorgram corresponding to binding of the Kunitz domain has been magnified in panel B.

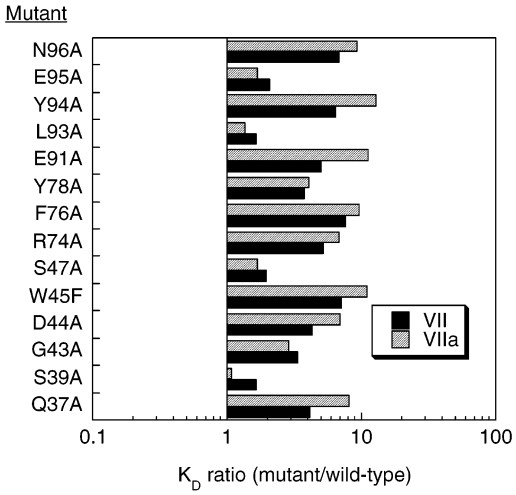

FIGURE 5: Effect of substitutions of sTF on the affinity for VII (black bars) or VIIa (hatched bars). Values are the ratios of the K_D values determined for the mutant relative to that of wild-type sTF.

comparable in magnitude (Figure 5). The decreased affinity for VII binding resulted mostly from a decreased on-rate (Table 2); decreased VIIa affinity was usually the result of both an increased off-rate and a decreased on-rate. In addition, data are included in Figure 5 for alanine substitution of two residues, Ser47 and Leu93, that do not contact VIIa in the TF−VIIa structure but are close to this region of interaction. Alanine substitution of these residues produced an insignificant change (<2-fold) in affinity for binding to both VII and VIIa.

DISCUSSION

Results of previous structure−function studies (*16*, *24*) indicated that the free energy of the binding of VIIa to TF is primarily contributed by interactions between the EGF-1 domain of VIIa and TF. The contribution to binding from the protease domain−TF interaction is more modest; however, this interface is critical for the allosteric linkage by which TF binding promotes the amidolytic and proteolytic activity of VIIa. Indeed, alanine substitution of Met164 in VIIa results in only a small loss in TF affinity but causes a dramatic decrease in the magnitude of the TF-dependent increase in the amidolytic and proteolytic activity of VIIa (*11*, *19*). In contrast, we find that mutations on the TF side of this interface mainly affect the affinity for VIIa but not the level of enzymatic activity upon saturation. Substitution of key residues in VIIa can disrupt the linkage between docking of the protease to TF and formation of the active site. The M164A mutant of VIIa (*11*, *19*) would appear to be less capable of assuming the conformation required for

full activity. Single-point mutations in TF do not appear to disrupt the allosteric linkage, suggesting that the active conformation of VIIa is not highly dependent on the specific contacts with TF side chains. The results are consistent with a model where TF promotes activity by selecting and stabilizing the active conformation of VIIa that is in equilibrium with one or more less active forms (*6*, *11*).

One difference from earlier work is our observation that the D44A mutant of TF does not cause a decrease in the maximal velocity of X activation upon saturation of VIIa with the cofactor. Gibbs et al. (*25*) showed that D44A sTF gave 50% of the maximal activity observed with wild-type sTF in a chromogenic peptide assay of VIIa activity. However, it is unclear whether concentrations of D44A sTF that were sufficiently high to saturate VIIa were used. Kelly et al. (*26*) observed a 7-fold decrease in the maximal rate of X activation for D44A compared to that for wild-type TF. Their assay used detergent-solubilized full-length TF, whereas our assay of X activation employed sTF in the presence of phospholipids. The presence of phospholipids may suppress the defect in cofactor function measured for D44A TF.

The SPR experiments show that VII and VIIa bind to sTF with similar kinetics and affinity. A contribution to the results from a significant level of VII activation during the binding experiments can be excluded for the following reasons. First, we depleted the VII preparation of active enzyme such that the trace levels of protease required for autoactivation were not present. Second, the anti-TF antibody 5G6 used to capture TF on the sensor chip surface inhibits VII autoactivation. Third, sTF is normally a poor cofactor for VII autoactivation in the absence of high concentrations of phospholipids or polylysine (*27*). The dextran matrix comprising the sensor chip has a net negative charge and thus would not be expected to mimic the effects on VII autoactivation observed for the positively charged polylysine. Finally, a significant level of Kunitz domain binding was only observed for the TF−VIIa surface, and not for TF−VII, consistent with a lack of VII activation during the binding experiments.

We have shown here that substitutions on the TF surface that contacts the protease domain of VIIa have nearly identical effects on the affinities for both VII and VIIa. The contact region on TF for the proteolytic domain of VII does not appear to extend beyond the region observed in the TF−VIIa structure since the S47A and L93A mutants of sTF did not impair binding to VII. Despite the steric clash implied by the modeling studies, the protease domains of both VII and VIIa seem to interact with the same surface on TF with nearly identical residue energetics. Two explanations for these results appear to be possible. Since the binding experiments did not employ an active site inhibitor, and because all of the reported structures for TF−VIIa complexes have inhibitors bound, the conformation of both VII and VIIa detected in the binding experiments may be different from that observed in the crystal structures. This model requires a secondary conformational change in the initial TF−VIIa complex for realization of full activity. VII would not be able to undergo this transition. This explanation appears to be unlikely since the pattern of changes in VIIa affinity with TF substitution is consistent with the side chain contacts observed in the TF−VIIa structure (*10*). For example, TF residue Tyr94 forms both hydrophobic and hydrogen bonding interactions with VIIa in the TF−VIIa complex structure, and alanine substitution of this residue causes a 12-fold decrease in affinity. The second explanation postulates that the VIIa conformation observed in the crystal structure of the TF−VIIa complex is the only one capable of high-affinity TF binding, and both VII and VIIa can readily assume this conformation. Since VII binds TF with kinetics and affinity comparable to those of VIIa, the energy barrier must be small between the active conformation and the conformation observed in the zymogen structure. Further changes in the active site related to the activation cleavage, and thus only accessible to VIIa and not VII, render the active enzyme. These additional changes in the active site could occur prior to or concomitant with TF binding. Given the good agreement between the structural and functional epitopes for VIIa binding, this second explanation is more consistent with the data.

The observation that VII and VIIa bind the same epitope on TF is consistent with earlier studies on the mechanism of VII autoactivation (*28*−*30*) and can be contrasted with the modes of binding predicted for substrates IX and X (*7*). Both IX and X, binding as substrates to the TF−VIIa complex, appear to interact with a portion of TF outside of the VIIa binding region. Since VIIa and VII bind to the same sites on TF, a TF−VIIa−VII ternary complex cannot be formed. Activation of VII bound to TF must be catalyzed by VIIa bound to a second molecule of TF. The kinetics of VII autoactivation on a membrane surface have previously been explained with a model in which a molecule of the TF−VII complex is the substrate for activation by a TF−VIIa complex (*29*). In addition, dimerization of sTF has been shown to promote autoactivation of VII (*30*). A common binding site on TF for both VII and VIIa is consistent with observations that VII can antagonize the activity of VIIa when TF is in limited supply (*31*). In the clinical situation where VIIa is used to treat bleeding disorders (*32*), enough VIIa must be provided to overcome the antagonism due to VII and restore normal bleeding times. The molecular details of how the TF−VIIa complex recognizes the TF−VII complex as a substrate await further experimentation.

ACKNOWLEDGMENT

We thank Mark Dennis for the gift of the IV-49-C Kunitz domain and Mark O'Connell for purification of VIIa. We are grateful for discussions with Dr. Robert Lazarus and for the continued support of Dr. Bart deVos.

REFERENCES

1. Nemerson, Y. (1988) Tissue factor and hemostasis, *Blood 71*, 1−8.
2. Davie, E. W., Fujikawa, K., and Kisiel, W. (1991) The coagulation cascade: initiation, maintenance, and regulation, *Biochemistry 30*, 10363−10370.
3. Bom, V. J., and Bertina, R. M. (1990) The contributions of Ca^{2+}, phospholipids and tissue-factor apoprotein to the activation of human blood-coagulation factor X by activated factor VII, *Biochem. J. 265*, 327−336.
4. Morrissey, J. H., Macik, B. G., Neuenschwander, P. F., and Comp, P. C. (1993) Quantitation of activated factor VII levels in plasma using a tissue factor mutant selectively deficient in promoting factor VII activation, *Blood 81*, 734−744.
5. Butenas, S., and Mann, K. G. (1996) Kinetics of human factor VII activation, *Biochemistry 35*, 1904−1910.
6. Higashi, S., Matsumoto, N., and Iwanaga, S. (1996) Molecular mechanism of tissue factor-mediated acceleration of factor VIIa activity, *J. Biol. Chem. 271*, 26569−26574.

7. Kirchhofer, D., Lipari, M. T., Moran, P., Eigenbrot, C., and Kelley, R. F. (2000) The tissue factor region that interacts with substrates factor IX and Factor X, *Biochemistry 39*, 7380−7387.
8. Neuenschwander, P. F., Branam, D. E., and Morrissey, J. H. (1993) Importance of substrate composition, pH and other variables on tissue factor enhancement of factor VIIa activity, *Thromb. Haemostasis 70*, 970−977.
9. Lawson, J. H., Butenas, S., and Mann, K. G. (1992) The evaluation of complex-dependent alterations in human factor VIIa, *J. Biol. Chem. 267*, 4834−4843.
10. Banner, D. W., D'Arcy, A., Chene, C., Winkler, F. K., Guha, A., Konigsberg, W. H., Nemerson, Y., and Kirchhofer, D. (1996) The crystal structure of the complex of blood coagulation factor VIIa with soluble tissue factor, *Nature 380*, 41−46.
11. Dickinson, C. D., Kelly, C. R., and Ruf, W. (1996) Identification of surface residues mediating tissue factor binding and catalytic function of the serine protease factor VIIa, *Proc. Natl. Acad. Sci. U.S.A. 93*, 14379−14384.
12. Eigenbrot, C., Kirchhofer, D., Dennis, M. S., Santell, L., Lazarus, R. A., Stamos, J., and Ultsch, M. H. (2001) The factor VII zymogen structure reveals reregistration of beta strands during activation, *Structure 9*, 627−636.
13. Kirchhofer, D., Eigenbrot, C., Lipari, M. T., Moran, P., Peek, M., and Kelley, R. F. (2001) The tissue factor region that interacts with factor Xa in the activation of factor VII, *Biochemistry 40*, 675−682.
14. Kirchhofer, D., Moran, P., Chiang, N., Kim, J., Riederer, M. A., Eigenbrot, C., and Kelley, R. F. (2000) Epitope location on tissue factor determines the anticoagulant potency of monoclonal anti-tissue factor antibodies, *Thromb. Haemostasis 84*, 1072−1081.
15. Dennis, M. S., and Lazarus, R. A. (1994) Kunitz domain inhibitors of tissue factor-factor VIIa. II. Potent and specific inhibitors by competitive phage selection, *J. Biol. Chem. 269*, 22137−22144.
16. Kelley, R. F., Costas, K. E., O'Connell, M. P., and Lazarus, R. A. (1995) Analysis of the factor VIIa binding site on human tissue factor: effects of tissue factor mutations on the kinetics and thermodynamics of binding, *Biochemistry 34*, 10383−10392.
17. Mimms, L. T., Zampighi, G., Nozaki, Y., Tanford, C., and Reynolds, J. A. (1981) Phospholipid vesicle formation and transmembrane protein incorporation using octyl glucoside, *Biochemistry 20*, 833−840.
18. Williams, E. B., Krishnaswamy, S., and Mann, K. G. (1989) Zymogen/enzyme discrimination using peptide chloromethyl ketones, *J. Biol. Chem. 264*, 7536−7545.
19. Dickinson, C. D., and Ruf, W. (1997) Active site modification of factor VIIa affects interactions of the protease domain with tissue factor, *J. Biol. Chem. 272*, 19875−19879.
20. Kelley, R. F. (1994) Thermodynamics of Protein−Protein Interaction Studied by Using Biacore and Single-site Mutagenesis, *Methods: A Companion to Methods in Enzymology*, Vol. 6, pp 111−120, Academic Press, San Diego.
21. Faelber, K., Kirchhofer, D., Presta, L., Kelley, R. F., and Muller, Y. A. (2001) The 1.85 Å resolution crystal structures of tissue factor in complex with humanized Fab D3h44 and of free humanized Fab D3h44: revisiting the solvation of antigen combining sites, *J. Mol. Biol. 313*, 83−97.
22. Neuenschwander, P. F., and Morrissey, J. H. (1992) Deletion of the membrane anchoring region of tissue factor abolishes autoactivation of factor VII but not cofactor function. Analysis of a mutant with a selective deficiency in activity, *J. Biol. Chem. 267*, 14477−14482.
23. Vincent, J. P., and Lazdunski, M. (1976) Pre-existence of the active site in zymogens, the interaction of trypsinogen with the basic pancreatic trypsin inhibitor (Kunitz), *FEBS Lett. 63*, 240−244.
24. Toomey, J. R., Smith, K. J., and Stafford, D. W. (1991) Localization of the human tissue factor recognition determinant of human factor VIIa, *J. Biol. Chem. 266*, 19198−19202.
25. Gibbs, C. S., McCurdy, S. N., Leung, L. L., and Paborsky, L. R. (1994) Identification of the factor VIIa binding site on tissue factor by homologous loop swap and alanine scanning mutagenesis, *Biochemistry 33*, 14003−14010.
26. Kelly, C. R., Schullek, J. R., Ruf, W., and Edgington, T. S. (1996) Tissue factor residue Asp44 regulates catalytic function of the bound proteinase factor VIIa, *Biochem. J. 315* (Part 1), 145−151.
27. Fiore, M. M., Neuenschwander, P. F., and Morrissey, J. H. (1994) The biochemical basis for the apparent defect of soluble mutant tissue factor in enhancing the proteolytic activities of factor VIIa, *J. Biol. Chem. 269*, 143−149.
28. Yamamoto, M., Nakagaki, T., and Kisiel, W. (1992) Tissue factor-dependent autoactivation of human blood coagulation factor VII, *J. Biol. Chem. 267*, 19089−19094.
29. Neuenschwander, P. F., Fiore, M. M., and Morrissey, J. H. (1993) Factor VII autoactivation proceeds via interaction of distinct protease-cofactor and zymogen-cofactor complexes. Implications of a two-dimensional enzyme kinetic mechanism, *J. Biol. Chem. 268*, 21489−21492.
30. Donate, F., Kelly, C. R., Ruf, W., and Edgington, T. S. (2000) Dimerization of tissue factor supports solution-phase autoactivation of factor VII without influencing proteolytic activation of factor X, *Biochemistry 39*, 11467−11476.
31. van't Veer, C., Golden, N. J., and Mann, K. G. (2000) Inhibition of thrombin generation by the zymogen factor VII: implications for the treatment of hemophilia A by factor VIIa, *Blood 95*, 1330−1335.
32. Hedner, U. (2000) NovoSeven as a universal haemostatic agent, *Blood Coagulation Fibrinolysis 11* (Suppl. 1), S107−S111.

BI035738I